Journal of Neurochemistry

JOURNAL OF NEUROCHEMISTRY | 2008 | 105 | 1582–1595 doi: 10.1111/j.1471-4159.2008.05238.x

Minocycline neuroprotects, reduces microglial activation, inhibits caspase 3 induction, and viral replication following Japanese encephalitis

Manoj Kumar Mishra and Anirban Basu

National Brain Research Centre, Manesar, Haryana, India

Abstract

Minocycline is broadly protective in neurological disease models featuring inflammation and cell death and is being evaluated in clinical trials. Japanese encephalitis virus (JEV) is one of the most important causes of viral encephalitis worldwide. There is no specific treatment for Japanese encephalitis (JE) and no effective antiviral drugs have been discovered. Studies indicate that JE involves profound neuronal loss as well as secondary inflammation caused because of cell death. Minocycline is a semisynthetic second-generation tetracycline that exerts anti-inflammatory and antiapoptotic effects that are completely separate from its antimicrobial action. Because tetracycline treatment is clinically well tolerated, we investigated whether minocycline protects against experimental model of JE. Intravenous inoculation of GP78 strain of JEV in adult mice results in lethal encephalitis and caused primarily because of neuronal death and secondary inflammation caused because of cell death. Minocycline confers complete protection in mice following JEV infection ($p < 0.0001$). Neuronal apoptosis, microglial activation, active caspase activity, proinflammatory mediators, and viral titer were markedly decreased in minocycline-treated JEV infected mice on ninth day post-infection. Treatment with minocycline may act directly on brain cells, because neuronal cell line Neuro2a were also salvaged from JEV-induced death. Our data suggest that minocycline may be a candidate to consider in human clinical trials for JE patients.

Keywords: apoptosis, Japanese encephalitis virus, microglia, minocycline, neuron.

J. Neurochem. (2008) **105**, 1582–1595.

Flavivirus are important human pathogens causing variety of diseases ranging from mild febrile illness to severe encephalitis and hemorrhagic fever. Among them, Japanese encephalitis virus (JEV), a neurotropic one commonly affects children and is a major cause of acute encephalopathy (Chen *et al.* 2002). JEV is active over a vast geographic area that includes India, China, Japan, and virtually all of South-East Asia. Approximately 3 billion people live in the JEV endemic area covering much of Asia with nearly 50 000 cases of Japanese encephalitis (JE) reported each year. Of these, about 10 000 cases results in fatality and a high proportion of survivors have serious neurological and psychiatric sequelae (Kaur and Vrati 2003). Therapy for JE is supportive and no clearly effective antiviral agents exist. Therefore, the search is on for compounds which is cheap, easily available and with no or tolerable side effects combined with a protective potential when administered several hours after infection.

Minocycline, a semisynthetic tetracycline, has demonstrated remarkably broad neuroprotective properties in experimental models of ischemic stroke, Huntington's disease, amyotrophic lateral sclerosis (ALS), traumatic brain injury, multiple sclerosis, Parkinson's disease, and diabetic retinopathy (Yrjanheikki *et al.* 1999; Chen *et al.* 2000; Sanchez Mejia *et al.* 2001; Popovic *et al.* 2002; Wu *et al.* 2002; Zhu *et al.* 2002; Krady *et al.* 2005). Minocycline was shown to possess antiapoptotic (neuroprotective) as well as antiviral and anti-inflammatory properties against human immunodeficiency virus-induced encephalitis (Zink *et al.* 2005). A very recent *in vitro* study indicates that minocycline inhibits West Nile virus (WNV) replication and apoptosis in human neuronal

Received October 10, 2007; revised manuscript received December 4, 2007; accepted January 9, 2008.

Address correspondence and reprint requests to Anirban Basu, National Brain Research Centre, Manesar, Haryana 122050, India. E-mail: anirban@nbrc.res.in

Abbreviations used: ALS, amyotrophic lateral sclerosis; ERK, extracellular regulated kinase; IL, interleukin; JE, Japanese encephalitis; JEV, Japanese encephalitis virus; LDH, lactate dehydrogenase; MAPK, mitogen-activated protein kinase; MOI, multiplicity of infection; N2a, Neuro2a cells; NeuN, neuronal nuclei; PBS, phosphate buffer saline; PI, propidium iodide; PKC, protein kinase C; PS, porcine stable kidney cells; RT, room temperature; TUNEL, terminal deoxynucleotidyl transferase-mediated dUTP nick-end label; WNV, West Nile virus.

cells (Michaelis *et al.* 2007). The mechanism of minocycline-mediated neuroprotection have been demonstrated to result, at least in part, from inhibiting release of cytochrome *c* from the mitochondria in a transgenic mouse model of ALS (Zhu *et al.* 2002). Additional effects have been ascribed to minocycline that include inhibition of caspase 1, 3, and inducible nitric oxide transcriptional up-regulation and activation, reactive microgliosis, and activation of p38 mitogen-activated protein kinase (MAPK) and down-regulation of proinflammatory cytokines (Nikodemova *et al.* 2006). All inhibitory properties of minocycline, other than microgliosis, likely result from inhibiting downstream events after cytochrome *c* release. Inhibition of reactive microgliosis is a direct effect of minocycline *in vitro* (Tikka *et al.* 2001). At present it is not clear whether *in vivo* inhibition of reactive microgliosis is a direct effect of minocycline or a secondary event resulting from inhibition of neuronal death.

We have recently shown that proinflammatory mediators released by activated microglia induces neuronal death in JE (Ghoshal *et al.* 2007). In this study, we show that minocycline at relatively low doses is very effective neuroprotective drug against an experimental model of JE even when the administration is started next day following viral inoculation, indicating a clinically relevant therapeutic time window for this tetracycline derivative. Furthermore, our results also suggested that minocycline rescue 70% of animals even in animals with established infection of JEV. In addition, we report that the beneficial effect is associated with reduction of (i) proinflammatory cytokines, (ii) active caspase 3 activity, (iii) microgliosis, (iv) viral titer, and (v) neuronal death. As minocycline is well tolerated, it represents a potential new therapeutic for preventing or controlling the neurological complications of JE.

Material and methods

Minocycline administration in an animal model of JE

Adult BALB/c mice (4–6 weeks) were used in all experimental procedures. Mice were randomly assigned to four groups: Control group (Control); only minocycline group (PBS + M); JEV infected group (JEV); JEV and Minocycline treated group (JEV + M). We used a previously described animal model of JE with slight modification (Vrati *et al.* 1999a,b). BALB/c mice of either sex were injected with 3×10^5 p.f.u. of JE virus of strain GP78 through tail-vein. Control animals received phosphate buffered saline (PBS). Twice daily dose of minocycline (Sigma, St Louis, MO, USA) of 22.5 or 45 mg/kg body weight was administered intraperitonealy (i.p.) next day after JEV infection and continued for 6 days. Groups of five mice were killed at ninth day post-infection time point either for tissue, protein or RNA. From fifth day onwards animals started to show symptoms of JE including restriction of movements, limb paralysis, poor pain response, whole body tremor, piloerection, and hindlimb paralysis. On the ninth day post-infection all animals succumb to death. Scoring for behavioral analysis was performed in a masked manner to avoid bias toward any one group of animals. In another set of study, we have administered minocycline at sixth day post-infection. At sixth day post-JEV infection all the animals showed distinct sign of clinical symptoms of JE. Minocycline were given for 15 days twice a day with a dose of 45 mg/kg body weight. All experiments were performed according to the protocol approved by the Institutional Animal Ethics Committee of National Brain Research Center (NBRC).

Virus titration

JEV was titrated by plaque formation on porcine stable kidney cells (PS) monolayers. PS cells were seeded in 35-mm dishes to form semi-confluent monolayers in about 18 h. Monolayers were inoculated with 10-fold dilutions of virus sample made in minimum essential medium containing 1% fetal calf serum and incubated for 1 h at 37°C with occasional shaking. The inoculum was removed by aspiration and the monolayers were overlaid with minimum essential medium containing 4% fetal calf serum, 1% low-melting-point agarose and a cocktail of antibiotic–antimycotic solution (Gibco, Invitrogen Corporation, Grassland, NY, USA) containing penicillin, streptomycin, and amphotericin B. Plates were incubated at 37°C for 3–4 days until plaques became visible. To allow counting of the plaques, the cell monolayer was stained with crystal violet after fixing the cells with 10% formaldehyde (Vrati *et al.* 1999b).

Immunohistochemsitry

Animals were perfused and the brains were processed for cryostat sectioning. To label activated microglia and neurons sections were incubated overnight at 4°C with rabbit anti-Iba-1 (1/500; Wako, Osaka, Japan) and mouse anti-neuronal nuclei (NeuN) (1 : 500; Chemicon, Temecula, CA, USA), respectively. After washes slides were incubated with appropriate secondary antibodies and following final washes, sections were coverslipped.

To identify dead cells in the brain sections *In situ* Cell Death Detection Kit, TMR red (Roche, Mannheim, Germany) were used (Mishra *et al.* 2007a). Briefly sections were washed three times with PBS then incubated in permeabilization buffer for 2 min and then incubated in terminal deoxynucleotidyl transferase-mediated dUTP nick-end label (TUNEL) mix (terminal deoxynucleotidyl transferase in storage buffer and TMR red labeled-nucleotide mixture in reaction buffer) for 1 h at 22°C. The slides were mounted with mounting media containing 4′,6-diamino-2-phenylindole. All the slides were viewed using a Zeiss Axioplan 2 Fluorescence microscope (Zeiss, Gottingen, Germany).

Cytokine bead array

The BD mouse cytokine bead array kits (mouse inflammation CBA kit; BD Biosciences, San Diego, CA, USA) were used to quantitatively measure cytokine levels in mouse brain tissue lysates; 50 μL of mouse inflammation standard and sample dilutions were used and the assay was performed according to the manufacturer's instructions and analyzed on the FACS Calibur (BD Biosciences; Swarup *et al.* 2007a).

Active-caspase 3 assay

The Fluorometric CaspACE™ Assay System was purchased from Promega (Madison, WI, USA) and used according to the manufacturers directions. Duplicate assays were performed for each sample.

Fluorescence was measured using a SpectraMAX Gemini EM (Molecular Devices, Sunnyvale, CA, USA) at an excitation wavelength of 360 nm and an emission wavelength of 460 nm. Caspase 3 enzyme activity was expressed as picomoles of caspase 3 liberated per milligram of protein per minute (Krady *et al.* 2005).

Immunoblot

The brain tissue from individual animals from all four different groups was dissected and processed for protein isolation. Twenty microgram of each sample was electrophoresed on polyacrylamide gel and transferred onto a nitrocellulose membrane. After blocking, the blots were incubated overnight at 4°C with primary antibodies against caspase 3 (BD pharmingen, San Diego, CA, USA), phospho-Jun-N-terminal kinase, extracellular regulated kinase (ERK), phospho-ERK, p38 MAPK (Cell-Signaling, Boston, MA, USA), and protein kinase C (PKC-α; Stressgen, Ann Arbor, MI, USA). After extensive washes in PBS–Tween, blots were incubated with appropriate secondary antibodies. The blots were again rinsed in PBS–Tween and processed for development using chemiluminescence reagent. The images were captured and analyzed using Chemigenius Bioimaging System (Syngene, Cambridge, UK). The blots were stripped and reprobed with anti-β-tubulin (1 : 1 000; Santa Cruz Biotechnology, Santa Cruz, CA, USA) to determine equivalent loading of samples.

Semi-quantitative RT-PCR

Total cellular RNA was isolated from individual animals from all four different groups as described previously (Basu *et al.* 2002). Oligonucleotide primer pairs against JEV and cyclophilin mRNAs (as an internal control) were checked for specificity using BLAST search and synthesized by Sigma (Bangalore, India). PCR was performed using the QIAGEN OneStep RT-PCR Kit (Qiagen Biosciences, Hamburg, Germany) according to the manufacturer's instructions and reactions were carried out on Genius Techne thermal cycler (Techne Ltd., Cambridge, UK). PCR parameters were established for each primer set to determine the optimal annealing temperature and cycle number for evaluation within the linear range of amplification. Amplification of the mRNA sequences for JEV and cyclophilin produced single bands that were of the size predicted from the reported sequences for these mRNAs (Table 1). PCR products were heat denatured and separated on 2% agarose gel. PCR products were separated on 2% agarose gel, stained with ethidium bromide, and photographed using GeneSnap software provided with Chemigenius Bioimaging System. Photographs were analyzed by GeneTools software provided with same Bioimaging system.

Infection of mouse neuroblastoma cell line with JE virus, LDH assay, and immunoblot

Mouse neuroblastoma Neuro2a cells (N2a) were plated in 12-well plate at a density of 3×10^5 cells/well in 1 mL of medium, and were cultured for 18 h. Cells were pre-treated for 1 h with minocycline at concentration of 20 μM in serum-free media and then incubated with JE virus at different multiplicity of infection (MOI) for 1 h. The virus was removed and the plates were then washed with 1x PBS to remove the unbound virus. The plates were further incubated in minocycline (20 μM) containing serum-free media at 37°C for next 24 h. Then the supernatant was used for lactate dehydrogenase (LDH) assay to measure cell death (Promega) as described earlier (Krady *et al.* 2005). For immunoblots, in another set of experiments N2a cells were plated. Following infection with JEV (MOI = 5) and subsequent minocycline treatment cells were processed for immunoblot analysis for Bax and Bcl-2 protein (1 : 1000 dilution, Santa Cruz Biotechnology). Immunoblots were performed as mentioned earlier.

For TUNEL assay N2a cells were plated at a density of 1×10^4 cells per well of eight well chamber slides in medium containing 1% fetal bovine serum and exactly same four groups were examined as earlier (see LDH section). Assay was performed as mentioned earlier in the Material and methods section.

Intracellular staining by flow cytometry for JEV antigen

Mouse neuroblastoma N2a cells were plated in six-well plate at a density of 5×10^5 cells/well in 3 mL of medium, and were cultured for 18 h. Cells were harvested in 1x PBS after the similar experiments as earlier mentioned (LDH assay). After two washes with 1x PBS, cells were first fixed with BD cytofix solution (BD Biosciences) for 15 min. Then permeabilized by resuspending in permeabilization buffer (BD Cytoperm plus; BD Biosciences) and incubated at 22°C for at least 10 min. Cells were washed twice in wash buffer (PBS containing 1% bovine serum albumin) then resuspended in wash buffer at 1×10^6 cells per 100 μL. Primary antibody (JEV Nakayama strain; Chemicon) were added in 1 : 100 dilutions and incubated for 30 min at 22°C. The cells were washed five times with wash buffer and pelleted. Then incubated with FITC-conjugated secondary antibody for 30 min. After three times wash with wash buffer, finally, samples were resuspended in 400 μL FACS buffer and analyzed. Samples were analyzed on a FACS Calibur. Fold change was calculated by dividing the median fluorescence intensity of the infected and minocycline treated sample by that of the control sample (Krutzik and Nolan 2003). The percentage of population was calculated after gating the populations on Dot plot in Cell Quest Software (BD Biosciences).

Measurement of mitochondrial membrane potential

Neuro2a cells were plated at subconfluent density. Twenty-four hours later, cells were infected with JEV (MOI 1 : 5) and treated with minocycline as mentioned earlier. Later, the cells were incubated with 5 μM JC-1 fluorescence dye (Molecular Probes, Eugene, OR, USA) for 30 min and washed with PBS pre-warmed at 37°C. Mitochondrial membrane potential was evaluated qualitatively under a Zeiss Axioplan 2 Fluorescence microscope (20× magnifications) using 568 nm filter (Swarup *et al.* 2007b).

Table 1 Primers used for RT-PCR experiments and expected size of amplified products

	Forward primer	Reverse primer	Product size (bp)
GP78	5′-TTGACAATCATGGCAAACGA-3′	5′-CCCAACTTGCGCTGAATAAT-3′	200
Cyclophilin	5′-CCATCGTGTCATCAAGGACTTCAT-3′	5′-TTGCCATCCAGCCAGGAGGTCT-3′	192

Cell death assay by annexin–propidium iodide staining

Neuro2a cells were infected with JEV and treated with minocycline as mentioned earlier. Cells were collected in 1x binding buffer (25 mM HEPES plus NaOH, pH 7.4, 140 mM NaCl, and 1 mM $CaCl_2$). The 100 μL of samples (1×10^5 cells) at predetermined time points are incubated with 5 μL each of FITC labeled annexin V and propidium iodide (PI) in the dark for 5–15 min at 20–25°C (ambient temperature). After adding 400 μL of binding buffer in each tube, the samples are analyzed by FACS Calibur (van Genderen *et al.* 2006).

Statistics

Statistical analysis was performed using SIGMASTAT software (SPSS Inc., Chicago, IL, USA). Data were compared between groups using a Student's *t*-test. The statistical significance of the treatment effect between the groups was assessed by a one-way ANOVA Fisher's *post hoc* test. Differences with $p < 0.05$ were considered significant.

Results

Minocycline confer complete protection to animal from JE

Minocycline treatment conferred complete protection to mice following JEV infection JEV ($p < 0.001$) (Fig. 1a). To assess whether the protective effects of minocycline was dose-dependent, we treated animals with half the fully protective minocycline dose (22.5 mg/kg i.p. twice a day) ($p < 0.003$). This dose only delayed the disease onset and progression but did not offer complete protection as observed when treated with a dose of 45 mg/kg dose (Fig. 1b). Infection with JEV

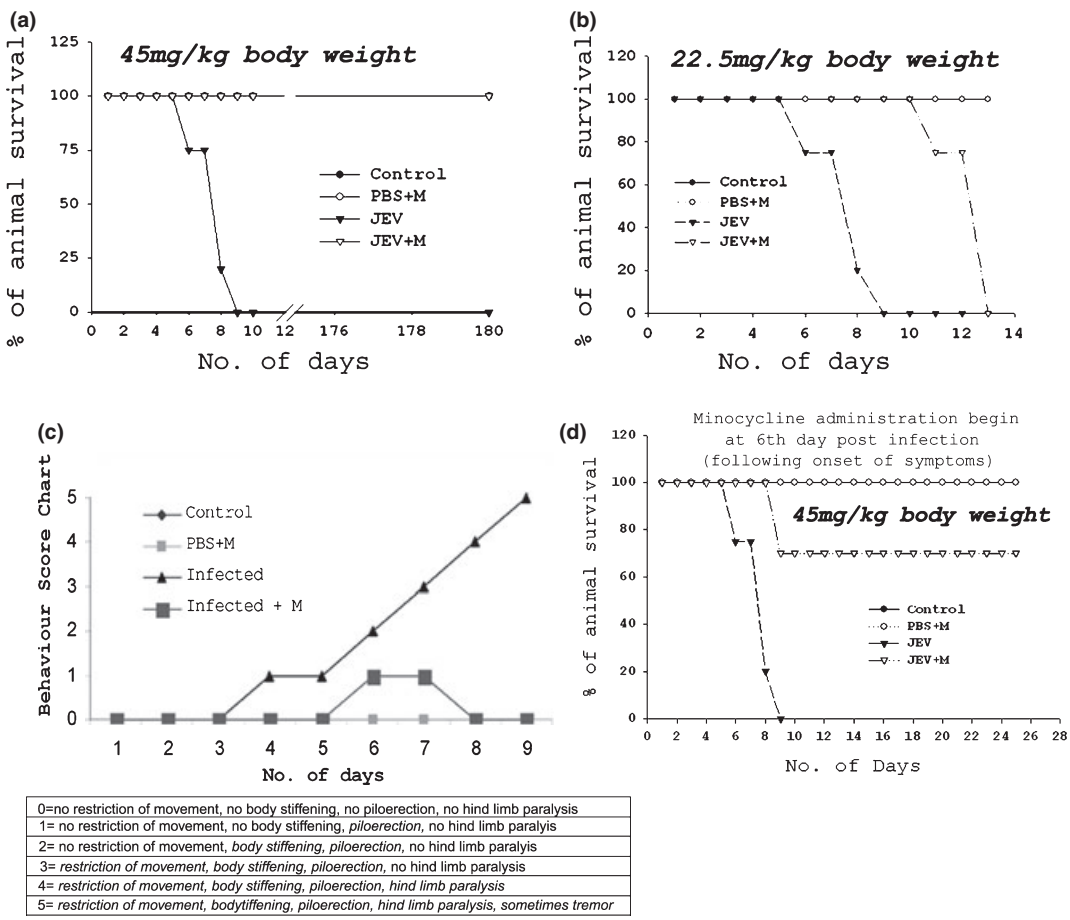

Fig. 1 Minocycline treatment confers complete protection to JEV infected mice: Survival of ($p < 0.0001$) mice infected with 3×10^5 p.f.u. of JEV was dramatically increased in groups that received minocycline (45 mg/kg body weights) treatment ($n = 15$ for each group) (a). Observation of animal survival experiments was performed in a masked manner to avoid bias toward any one group of animals. Minocycline at a dose of 22.5 mg/kg body weight only delayed the mortality of animals following JEV infection ($p < 0.003$) (b). Behavior score chart showing the gradual progression in disease after JEV infection (c) and minocycline treatment (45 mg/kg body weights) successfully abrogated that. Survival of mice infected with 3×10^5 p.f.u. of JEV was drastically increased in groups that received minocycline from sixth day post-infection (45 mg/kg body weight) treatment ($n = 10$ for each group) (d). Observation of animal survival experiments was performed in a masked manner to avoid bias toward any one group of animals. Minocycline administered after onset of symptoms (JE) also shows significant protection as 70% animals were survived ($p < 0.001$).

was accompanied with distinct symptoms and treatment with minocycline following virus infection, prevented animals from suffering. This effect of minocycline was clearly evident from the scoring of symptoms from different groups of animal (Fig. 1c). When treatment of minocycline started from sixth day post-infection (after onset of encephalitic symptoms) with a dose of 45 mg/kg body weight were also effective, as 70% animals were rescued from JEV-induced death (Fig. 1d).

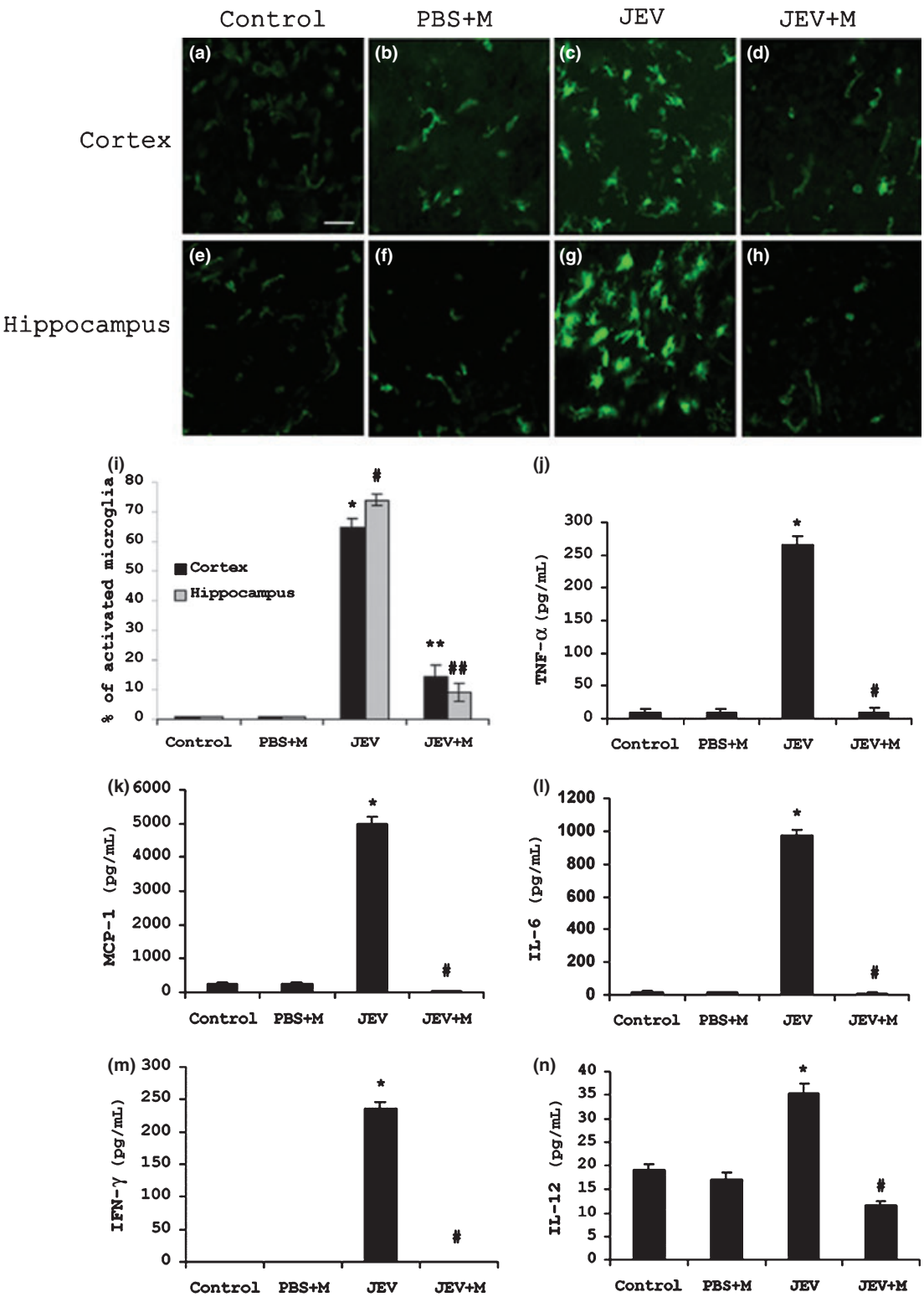

Minocycline abrogates microglial activation and induction of proinflammatory cytokines

To determine the role of minocycline in microglial activation, we stained brain sections with Iba-1. In the brain of JEV infected animal without treatment, the number of star-shaped 'activated' microglia (Fig. 2) appeared to be more frequent in the cortex Fig. 2c) and hippocampus (Fig. 2g) when compared with minocycline treated one. Iba-1 positive activated microglia were counted and plotted as a graph (Fig. 2i). Values represent the mean ± SEM from five random fields in three animals in each group. The increased expression of proinflammatory mediators [tumor necrosis factor-α, monocytes chemoattractant protein-1, interleukin-6 (IL-6), interferon-γ, and IL-12] observed following JEV infection was decreased to a large extent after minocycline treatment ($p < 0.0001$) (Fig. 2j–n). Data represent mean ± SEM of five animals from each group.

Treatment with minocycline can prevent JEV-induced neuronal death

To further characterize minocycline's effects on neuronal death, we assessed the ability of systemic minocycline treatment to animal following JEV infection. Figure 3 shows representative field from brain sections of control, only minocycline treated, JEV infected, and JEV infected but minocycline treated animals. The tissue sections were stained for NeuN to assess extent of neuronal death in the cortex (Fig. 3a–d) and hippocampus (Fig. 3e–h). Numerous healthy cells were observed in sections obtained from control brain when compared with JEV infected one. Minocycline treatment dramatically rescued the loss of neuronal health that was observed following viral infection. NeuN-positive cells of cortex were counted and plotted as a graph (Fig. 3q). Values represent the mean ± SEM from five random fields in three animals in each group (**$p < 0.001$). Similar results were observed when tissue sections were processed for TUNEL assay in the cortex (Fig. 3i–l) and hippocampus (Fig. 3m–p). There was a profound increase in TUNEL-positive cells in JEV infected animal when compared with control (*$p < 0.001$). TUNEL-positive cells of cortex were counted and plotted as a graph (Fig. 3r). Values represent the mean ± SEM from five random fields in three animals in each group (**$p < 0.001$). The results obtained from NeuN staining and TUNEL assay clearly indicates that JEV infection adversely affects neuronal viability ultimately culminating in neuronal loss, and minocycline treatment reversed this loss significantly.

Protein lysates from the whole brain of control, minocycline, JEV infected, and JEV infected and minocycline treated mice were used to perform western blots for active caspase 3, Bax, Bcl-2, and also assayed for caspase 3 activity as an index of apoptosis. There was a profound increase in active caspase 3 and Bax expression in JEV infected mice when compared with control and expression of both the protein was significantly down-regulated in animals those received minocycline following infection. The expression of Bcl-2 was reduced in infected brain compared with control and minocycline treatment increased the expression of this antiapoptotic protein (Fig. 3s). The Bax/Bcl-2 ratio high in infected brain (Fig. 3t) and minocycline treatment significantly reduced this effect (**$p < 0.001$). Active caspase 3 activity was increased more than fivefold within the CNS after infection compared with control animals (Fig. 3u). Minocycline treatment significantly abrogated the increase in caspase 3 activity (**$p < 0.001$). These experiments demonstrated that treatment with minocycline in JE could significantly rescue neuronal apoptosis and signaling events associated with cell death.

Minocycline modulate the expression pattern of several key proteins associated with stress

Western blot analysis demonstrated a significant inhibition in the expression of different stress related proteins whose levels were elevated following JEV infection, upon minocycline treatment (Fig. 4a). There was a significant increase in the expression of phospho-p38 MAPK (15-fold), phospho-Jun-N-terminal kinase (13-fold), and phospho-ERK (14-fold) in JEV infected mice when compared with control. But minocycline treatment dramatically reduced their level. Interestingly, the significant decrease in phospho-PKC-α expression following JEV infection was up-regulated in JEV infected animals that received minocycline treatment (Fig. 4a and b; $p < 0.01$).

Fig. 2 Inhibition of microglial activation and reduction in proinflammatory mediators after treatment with minocycline following JEV infection. Minocycline treatment of infected mice results in inhibition of activated microglia by a decrease in Iba-1 expression in them. Immunohistochemical staining for Iba-1 was used to detect the activated microglia in cortex (a–d) and hippocampus (e–h) of the brain tissue (40× magnification) sections from control, only minocycline, JEV-infected, and JEV infected and minocycline treated animals at 9 days post-infection. Iba-1 positive activated microglia were counted and plotted as a graph (i). Values represent the mean ± SEM from five random fields in three animals in each group ($^{*/\#}p < 0.001$, relative to control in cortex and hippocampus, respectively) and ($^{**/\#\#}p < 0.001$, relative to JEV infected animals in cortex and hippocampus, respectively). Scale bar: 25 μm. Cytokine bead array expression for proinflammatory mediators also showed profound decrease in (j) tumor necrosis factor-α (TNF-α), (k) MCP-1, (l) IL-6, (m) interferon-γ (IFN-γ), and (n) IL-12 levels after minocycline treatment ($^{*}p < 0.001$ relative to control and $^{\#}p < 0.0001$ relative to JEV infected mice). Data represent mean ± SEM of five animals from each group.

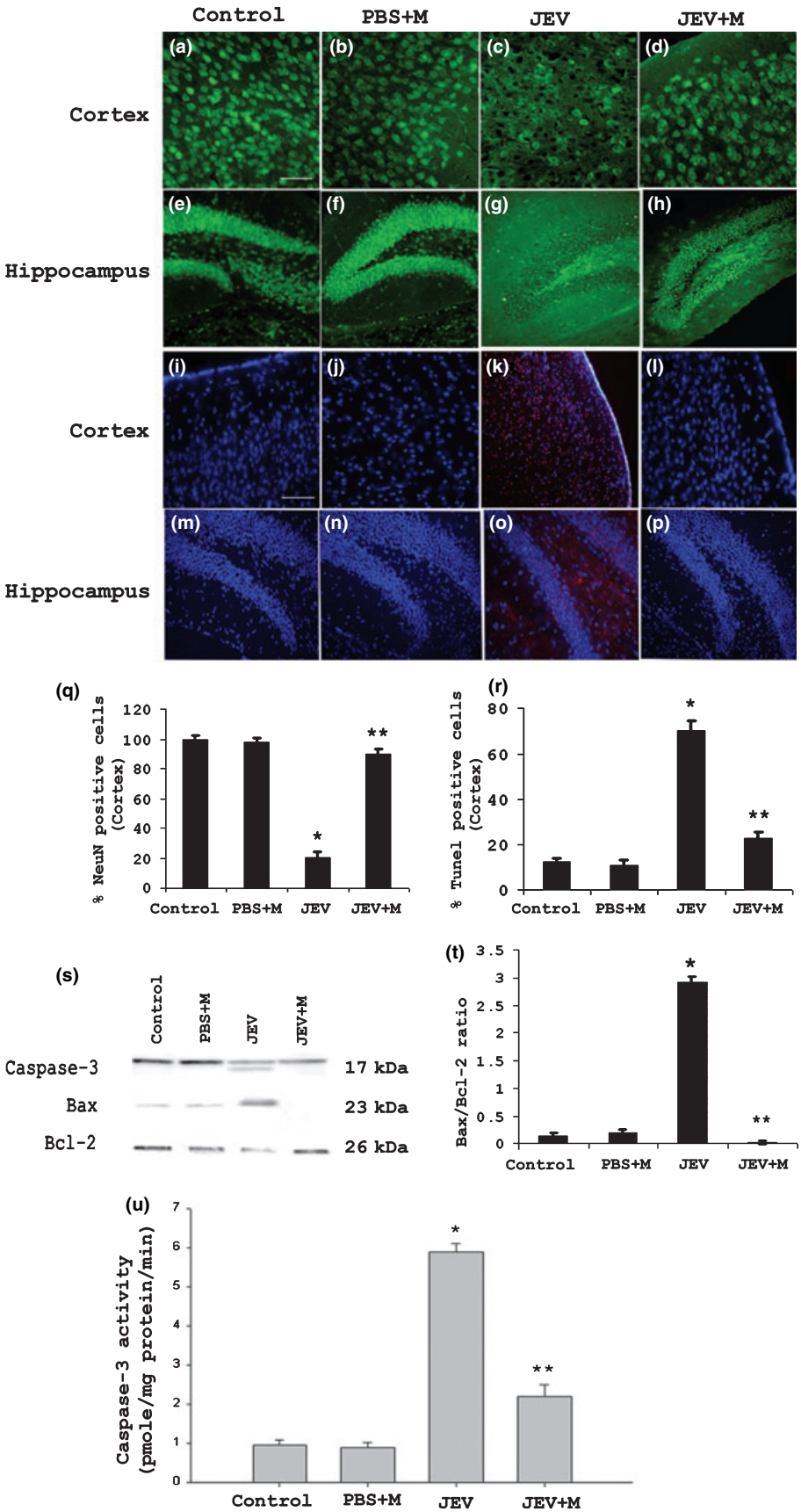

Minocycline treatment reduce the viral titer and mRNA transcripts of JEV *in vivo*

Virus isolated from JEV infected animal brain was titrated by plaque formation on PS monolayers. Treatment with minocycline significantly reduced the virus titers in JEV infected animals (1.5×10^5 p.f.u./mL in JEV infected mice and after treatment it reduced to 2.5×10^2 p.f.u./mL (Fig. 5a). There was a significant and dramatic decrease in JEV viral titer after minocycline treatment ($p < 0.001$). We performed semi-quantitative RT-PCR to assess the mRNA transcript level of JEV in the brain following infection and after minocycline treatment. Minocycline treatment significantly reduced the JEV mRNA level at 9 days post-infection. (Fig. 5b and c; $p < 0.005$). Some animals observed for long-term effect of minocycline on viral titer in JEV infected mice and were killed after sixth month of infection ($^{\#}p < 0.001$) represented as JEV + M1 group.

Minocycline treatment reduces the intracellular viral load and mRNA transcripts of JEV *in vitro*

To assess whether minocycline could prevent intracellular viral load and mRNA transcript, we co-cultured JEV with N2a cell lines for 24 h. Then intracellular staining of JEV was performed by flow cytometer in mouse neuronal cell line (N2a); the JEV infected cells were 61.55% whereas after minocycline treatment it comes down to 37.33% of the total cells population (Fig. 6a). We performed semi-quantitative RT-PCR to assess the mRNA transcript level of JEV after infection in cells and after minocycline treatment. Minocycline treatment significantly reduced the level of JEV mRNA transcript in N2a cells (Fig. 6b and c; $p < 0.001$).

Minocycline prevents JEV-induced neuronal apoptosis

To determine whether minocycline could prevent JEV-induced neurotoxicity, we co-cultured JEV with N2a cell lines for 24 h. Treatment with minocycline significantly reduced the effects of JEV-induced cytotoxicity of N2a cells. After 24 h, cell supernatants were assayed for LDH as a measure of cell death (Fig. 7a) and cells were observed for

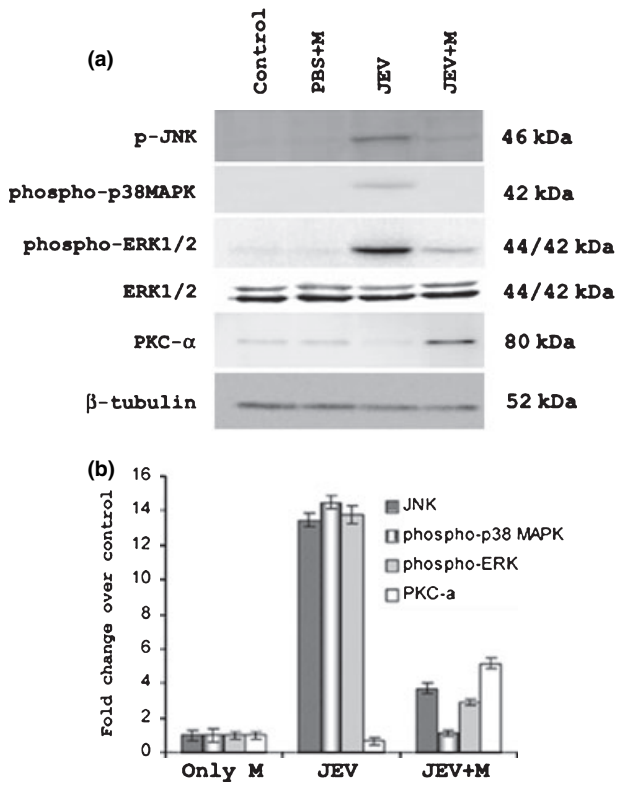

Fig. 4 The effect of minocycline following JEV infection *in vivo* on the expression of phospho-JNK, phospho-p38 MAPK, phospho-ERK, ERK1/2, and phospho-PKC-α. Representative (one individual animal from each group) western blot analysis demonstrating the induction of phospho-p38 MAPK, phospho-JNK, and phospho-ERK in JEV infected mice and minocycline treatment inhibits their expression. On the other hand, there is a reduction in phospho-PKC-α in JEV infected mice and minocycline treatment reverse the expression profile (a). There is no change in ERK1/2 in control, infected and minocycline group of animals. The increased expressions were in phospho-p38 MAPK, phospho-JNK, and phospho-ERK and reduced expression in phospho-PKC-α in JEV infected mice compared with control (b), $p < 0.01$. Blots were reprobed for β-tubulin to establish equal protein loading. Data represent mean ± SEM of five animals from each group.

Fig. 3 Minocycline attenuates virus-induced neuronal death in the CNS. The total number of NeuN-positive cells is significantly decreased in JEV infected mice when compared with control and JEV infected but minocycline treated mice in cortex (a–d) and hippocampus (e–h). NeuN-positive cells of cortex were counted and plotted as a graph (q). Values represent the mean ± SEM from five random fields in three animals in each group ($^{**}p < 0.001$). The total number of TdT-mediated dUTP nick-end label (TUNEL)-positive cells are significantly reduced in the brains of minocycline treated mice when compared with JEV infected mice (i–p). TUNEL-positive cells of cortex were counted and plotted as a graph (r). Values represent the mean ± SEM from five random fields in three animals in each group ($^{**}p < 0.001$). Visible band for active caspase 3 was observed in protein sample isolated from JEV infected animal(s). Treatment with minocycline following JEV infection completely abolished the active caspase 3 band. Increased expression of Bax and decreased level of Bcl-2 were observed in JEV infected samples compare with minocycline treated group. The Bax/Bcl-2 ratio high in infected brain (t) and minocycline treatment significantly reduced this effect ($^{**}p < 0.001$). Active caspase 3 activity measurements also indicate profound increase in caspase 3 activity in JEV infected mice (u). This activity has been significantly decreased in JEV infected but minocycline treated animals compared with infected animals. Data represent mean ± SEM of five animals from each group. $^{**}p < 0.001$ relative to infected animals. $^{*}p < 0.01$ relative to control. Scale bar: 50 μm.

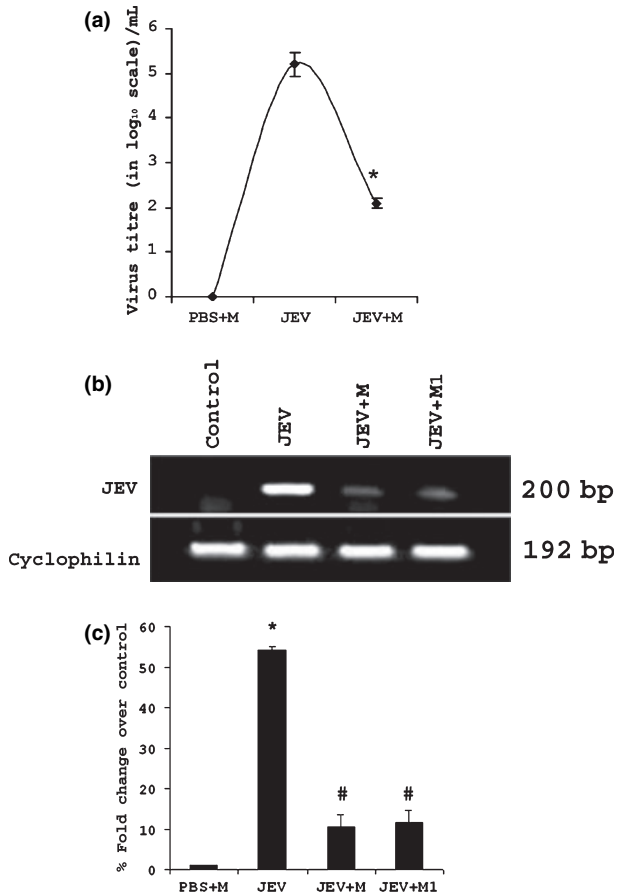

Fig. 5 Minocycline reduced the CNS viral load following JEV infection *in vivo*: JEV was titrated by plaque formation on PS monolayers. PS cells were seeded in 35-mm dishes to form semi-confluent monolayers in about 18 h. Monolayers were inoculated with 10-fold dilutions of virus sample made in MEM containing 1% FCS and incubated for 1 h at 37°C with occasional shaking. Plates were incubated at 37°C for 3–4 days until plaques became visible. To allow counting of the plaques, the cell monolayer was stained with crystal violet after fixing the cells with 10% formaldehyde. The viral titer obtained after ninth day post-infection of JEV was 1.5×10^5 p.f.u. (a) and minocycline dramatically decreases the viral titer upto 2×10^5 p.f.u. ($^*p < 0.001$). The mRNA transcript of virus was also increased after mice challenge with JEV ($^*p < 0.001$) and minocycline dramatically abrogate the virus replication (b and c) ($^{\#}p < 0.005$). JEV + M1 represents, the animals observed for long-term effect of minocycline on viral titer in JEV infected mice and were killed after sixth month of infection ($^{\#}p < 0.001$). Data represent mean ± SEM of five animals from each group.

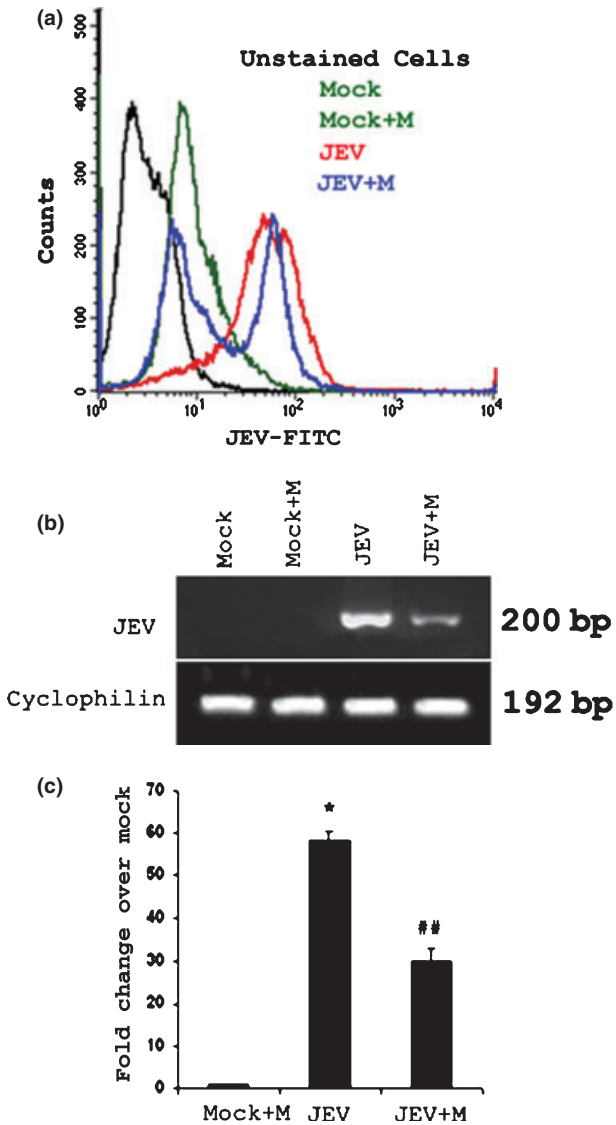

Fig. 6 Minocycline reduced the viral load in Neuro2a cells following JEV infection *in vitro*: Neuro2a cells were pre-treated for 1 h with minocycline at concentration of 20 μM in serum-free media. Cells were then incubated with JE virus at different multiplicity of infection (MOI) for 1 h. The virus was removed and the plates were then washed with 1x PBS to remove the unbound virus. The plates were further incubated in minocycline (20 μM) containing serum-free media at 37°C for next 24 h. Intracellular staining for JEV specific viral protein in N2a cells shows higher amount of viral protein following infection (Red Line) (a). Minocycline treatment significantly reduces the JEV specific protein in N2a cells (Blue line) ($p < 0.001$). The viral transcript levels in N2a cells were quantified after JEV infection (b and c). After JEV infection for 24 h, there was a robust increase in its transcript level and minocycline treatment reduced this significantly robustly ($^{\#\#}p < 0.001$). Data represent mean ± SEM of three individual experiments. $^*p < 0.01$ relative to control.

cytopathic effects (Fig. 7b–e), fixed, and processed for TUNEL as an index of apoptotic and necrotic cell death (Fig. 7f–I). Minocycline treatment conferred significant protection from JEV-induced cell death. Even with a MOI of 10 minocycline inhibited 50% neuronal death. A dramatic increase in TUNEL-positive cells was observed when N2a cells were co-cultured with JEV. Again, treatment with minocycline significantly rescued neuronal cell death.

We further investigated the mechanism behind the observed reduction in cell death in minocycline treated group. As JEV infection induces mitochondrial dependent apoptosis, we elucidated the role of mitochondrial potential in minocycline treated samples, using the cationic dye JC-1 that signals the loss of mitochondrial potential in apoptotic cells. Apoptotic cells can be identified by a decrease in JC-1 red fluorescence and an increase in JC-1 green fluorescence in the cytoplasm. The mock infected and minocycline treated N2a cells had predominant red fluorescence (Fig. 7j and k, respectively). JEV infected cells had disrupted mitochondrial potential as indicated by increased green fluorescence (Fig. 7l). However, JEV infected and minocycline treated N2a cells had reduced damage of mitochondrial integrity as shown by red fluorescence (Fig. 7m).

We also evaluated the necrotic and late apoptotic populations by annexin–PI staining. Flow cytometry of the N2a cell suspension produces an annexin V versus PI dot plot with living cells (annexin V- and PI-negative), living cells with a compromised membrane as a result of scraping (annexin V-negative and PI-positive), early apoptosis (annexin V-positive and PI-negative), and late apoptosis or necrosis (annexin- and PI-positive). After JEV infection 73% N2a cells were annexin V- and PI-positive, showing robust necrosis and late apoptosis following JEV infection (Fig. 7p). The minocycline treatment reduced this effect drastically and only 21.39% cells were annexin V- and PI-positive (Fig. 7q). This result suggests that minocycline rescues JEV infected N2a cells from apoptosis and necrosis by preserving mitochondrial integrity. Western blot showing significant increase in Bax and decrease in Bcl-2 expressions in N2a cells after JEV infection when compared with control (Fig. 7s). Minocycline treatment significantly reversed the expression pattern of Bax and Bcl-2 in JEV infected N2a cells.

Discussion

The antibiotic minocycline has been shown to have neuroprotective properties in diverse models of neurodegeneration and CNS injury (Arvin *et al.* 2002; Kriz *et al.* 2002; Zhu *et al.* 2002); (Thomas *et al.* 2003); (Du *et al.* 2001); (Van Den Bosch *et al.* 2002); (Tikka *et al.* 2001);(Hirsch *et al.* 2003); (Krady *et al.* 2005); (Yrjanheikki *et al.* 1998); (Fan *et al.* 2007). However, until recently this drug had not been tested in experimental models of CNS infection. It has been previously reported that minocycline protects infected mice from neuroadapted Sindbis virus-induced spinal motor neuron death (Darman *et al.* 2004). Another study demonstrated that the treatment of reovirus-infected neonatal mice with minocycline delays mortality of the resulting encephalitis (Richardson-Burns and Tyler 2005). A recent study indicates that therapy with minocycline aggravates experimental rabies in mice (Jackson *et al.* 2007). Another finding suggests that minocycline protects detrimental host immune responses of mice from fatal alpha virus encephalitis (Irani and Prow 2007) and finally a very recent study reported the effect of minocycline on viral titer and neuronal apoptosis in WNV (Michaelis *et al.* 2007).The major finding in this study is that treatment with minocycline provides a complete protection against experimental JE. Minocycline's neuroprotective action is associated with marked decreases in (i) neuronal apoptosis, (ii) the level of active caspase, (iii) microgliosis, (iv) viral titer, and (v) the level of proinflammatory mediators. Furthermore, treatment with minocycline also improves the behavioral outcome following JE.

We showed previously that the increased microglial activation following JEV infection influences the outcome of viral pathogenesis and it is likely that the increased microglial activation triggers bystander damage, as the animals eventually succumb to death (Ghoshal *et al.* 2007). Inhibition of chronic neuroinflammation, particularly of microglial activation, has been suggested to be a practical strategy in the treatment of neurodegenerative diseases. We show here that the treatment with minocycline following JE reduces the number of activated microglia as well as the level of proinflammatory cytokines IL-6, tumor necrosis factor-α, interferon-γ, IL-12p70, and chemokine monocytes chemoattractant protein-1. These data further support that microglial activation and subsequent inflammation is critical in determining the outcome of viral pathogenesis observed in JE.

The dose of minocycline that was used in these animals (45 mg/kg, twice daily) is within in the tolerated range of humans. It can be difficult to compare effective or toxic doses from one species to another. Two double-blind, randomized, placebo-controlled feasibility trials of minocycline in patients with ALS have been reported few years back (Gordon *et al.* 2004). In the first, 19 patients were treated with 200 mg/day of minocycline for 6 months with no difference in adverse events compared with those in the placebo group. In second, 23 patients received up to 400 mg/day in an 8-month crossover trial. The mean tolerated dose in this study was 387 mg/day. These findings suggest that minocycline at the dose that suppressed CNS inflammation, neuronal apoptosis, and virus replication in animal may be well tolerated in JEV-infected individuals.

We have recently reported that JEV infection is also accompanied by profound neuronal apoptosis (Mishra *et al.* 2007b). In addition to its direct actions on microglia, minocycline also has been shown to exert antiapoptotic effects by inhibiting caspases 1 and 3, and inhibiting the release of cytochrome *c* from mitochondria (Chen *et al.* 2000); (Sanchez Mejia *et al.* 2001); (Wang *et al.* 2003); (Zhu *et al.* 2002). These actions likely contributed to our *in vivo* finding of reduced caspase 3 activity as well as our *in vitro* findings with N2a cell line showing reduced apoptosis. These data suggest that minocycline is also working as an antiapoptotic molecule in this model of infection. The

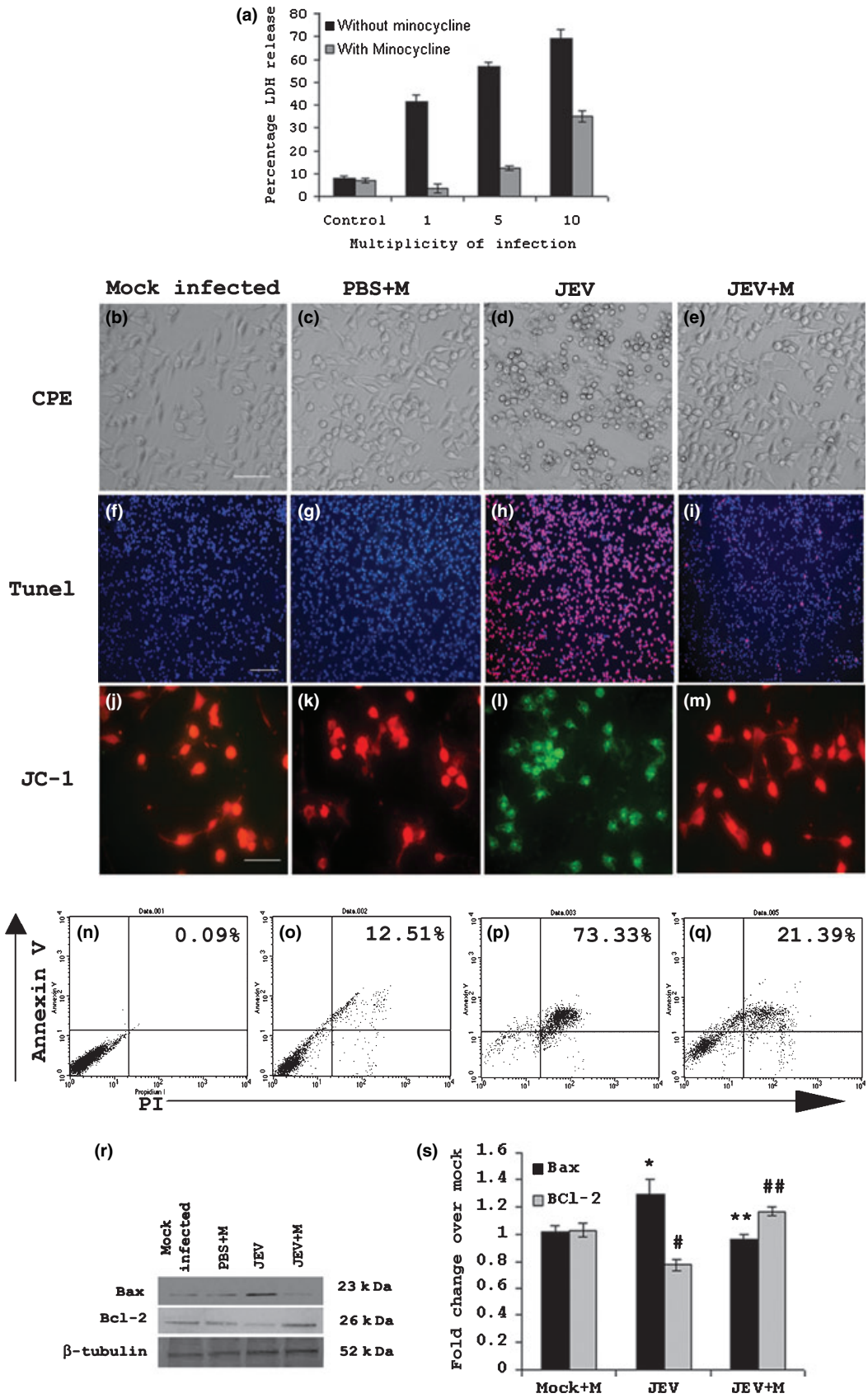

Fig. 7 Minocycline prevents JEV-induced neuronal cell death: Neuro2a cells were pre-treated for 1 h with minocycline at concentration of 20 μM in serum-free media. Cells were then incubated with JE virus at different multiplicity of infection (MOI) for 1 h. The virus was removed and the plates were then washed with 1x PBS to remove the unbound virus. The plates were further incubated in minocycline (20 μM) containing serum-free media at 37°C for next 24 h. JEV infected Neuro2a cells show significant increase in release of LDH compared with mock infected cells and after pre- and post-treatment with minocycline (20 μM) show significant reduction in LDH release, compared with only JEV infected N2a cells (a). Data represent mean ± SEM from three independent experiments performed in duplicate ($p < 0.001$). JEV-induced formation of cytopathic effects (CPE) as characterized by cell rounding and detachment. The minocycline treatment rescues the cells from CPE (b–e). TUNEL assay of mouse neuronal cells (N2a), showing TUNEL-positive cells (red) co-localized with DAPI. Negligible cell death was observed in control whereas profound increase in the number of TUNEL-positive cells seen when N2a was co-cultured with JE virus. Moreover, almost negligible TUNEL-positive cells were seen in JEV infected but minocycline treated cells. A dramatic decrease in TUNEL-positive cells was noted, indicating antiapoptotic and antinecrotic role of minocycline (f–i). From similar experiments, as mentioned above then N2a cells were subjected to JC-1 staining to study the changes in the mitochondrial membrane potential. JC-1 specifically detects the polarized mitochondria as red, and the depolarized membrane becomes green (j–m). The JEV infection profoundly decreased the mitochondrial membrane potential as evident from the loss of red mitochondrial staining. Flow cytometry analysis showing annexin–PI-positive cells were profound in JEV infected N2a cells and the minocycline treatment inhibits these effects significantly (n–q; $p < 0.001$). Upper right quadrants are showing cell population with late apoptosis/necrosis. As evident from dot blot analysis around 73% cells were late apoptotic/necrotic after JEV infection; minocycline reverses these effects dramatically. One representative experiment out of three is shown. Western blot showing Bax and Bcl-2 expressions in N2a cells after JEV co-culture for 24 h (r–s). Minocycline significantly reverses these effects ($^{**}p < 0.01$) and ($^{\#\#}p < 0.005$). Data represent mean ± SEM from three independent experiments performed in duplicate. Scale bar: 50 μm. $^{*/\#}p < 0.01$ relative to control.

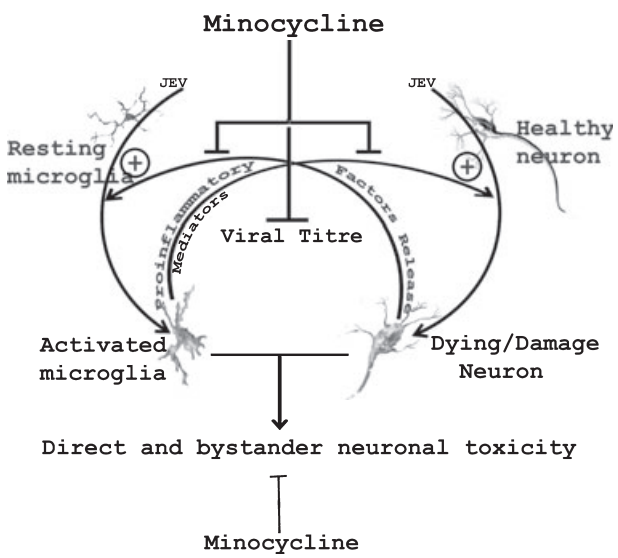

Fig. 8 Schematic diagram depicting neuron–microglia interaction following JEV infection: Neuron–microglia interaction following JEV infection originally adapted from Hald and Lotharius (2005). Minocycline has direct effect on intracellular JEV replication. Neurons whose viability has been compromised by JEV infection may release factors that activate resting microglia. Furthermore activated microglial released proinflammatory mediators may induce or exacerbate neuronal toxicity. This could result in direct and bystander neurotoxicity. Minocycline's anti-inflammatory, antiapoptotic and antiviral effects are beneficial in reducing the neuronal death induced by JEV. Blunt arrows indicate pathways that are inhibited by minocycline (Fig. 8).

modulation of apoptosis by minocycline could be because of its effects on apoptogenic molecules such as caspase in concert with its promotion of Bcl-2. *In vivo* microglial activation could be a response to neuronal damage with the subsequent inflammation resulting in negative consequences. Henceforth, early inhibition of neuronal apoptosis compound with a decrease in the subsequent release of proinflammatory mediators by activated microglia would attenuate the severity of disease observed in JE. Because minocycline's both anti-inflammatory and antiapoptotic effects will be beneficial in reducing the severity of diseases induced by JEV, our finding provides compelling evidence to support the administration of minocycline for treating JE patients. Furthermore, our results also suggested that minocycline rescue 70% of animals even in animals with established infection of JEV. JE is often accompanied by several neurological sequeale including severe movement disorders. To determine whether the preservation of brain tissue correlated with a preservation of neurological function, we used wire-hang test as a measure of motor neuron function. We observed significant improvement in the behavior of JEV infected versus JEV infected but minocycline treated mice in this test (*data not shown*).

We have found that JEV infections down-regulate the level of PKC-α, and treatment with minocycline reverses it in a significant extent. The decrease in the activity of PKC suggests that intracellular cAMP levels may be down-regulated, and it is also consistent with the level of apoptosis. In an interesting study it was reported earlier that cAMP protects against Staurosporine and Wortmannin induced neuronal apoptosis (Goswami *et al.* 1998). Staurosponne was initially described as an inhibitor of PKC but was then discovered to activate a specific 60-kDa serine/threonine kinase and has since been used to induce apoptosis in a range of cells from chondrocytes and oligodendrocytes to embryonic neurons (Wiesner and Dawson 1996a) and neuroblastoma cell lines (Wiesner and Dawson 1996b). Staurosporine may directly activate the caspases that cause degradation of

poly (ADP-ribose) polymerase and lamins and ultimately cell death or may work through inhibition of the antiapoptotic kinase, PKC, which is believed to phosphorylate Bad and prevent it from inactivating the protective proteins of the Bcl-2 family (Ito *et al.* 1997). It is highly possible that JE virus may be exploiting the same pathway to induce neuronal death and minocycline inhibiting this cell death cascade by up-regulating PKC, the antiapoptotic kinase. However more research is necessary to derive any firm conclusion.

Perhaps, the most unexpected result of these studies was the ability of minocycline to substantially inhibit replication of JEV. A very recent study describing minocycline inhibition of WNV in human neuronal cells was recently reported (Michaelis *et al.* 2007). Compared with anti-inflammatory or antiapoptotic property, minocycline's antiviral effect is relatively new phenomena. Another very recent studies indicate that minocycline has antiviral property against human immunodeficiency virus (Zink *et al.* 2005). Moreover, WNV and JEV belong to same family of viruses. These two recent studies prompted us to evaluate the antiviral role of minocycline in JE. Our study clearly indicates the antiviral role of minocycline against JEV. Therefore, individual suffering from severe encephalitis induced by JEV may benefit from minocycline by antiviral effects and by neuroprotective and anti-inflammatory effects that are independent of antiviral activity. It seems unlikely that minocycline has classic antiviral activity, as do reverse transcriptase and protease inhibitors because the antibiotic was not engineered to target a specific viral protein.

We propose that rather than exerting direct antiviral activity, minocycline modifies the intracellular or extracellular environment making it non-permissive for JEV replication. The ability of minocycline to modify environments differentially in primary macrophages and T lymphocytes (as evidenced by the differential effect of minocycline on p38 activation) raises the possibility that each cell type has a unique mechanism of suppression (Cohen *et al.* 1997; Shapiro *et al.* 1997; Darcissac *et al.* 2000). An important potential therapeutic advantage of this differential effect is that if the virus develops mutations that confer resistance to minocycline in one target cell type, that resistance might not confer a replicative advantage in the other cell type.

Minocycline is a safe drug commonly used for prolonged treatment of infections, rheumatoid arthritis, and acne vulgaris (Chopra 2001). Our data support, minocycline, which is in clinical trials for both Parkinson's disease and Huntington's disease, may be a an ideal candidate for considering in a human trial for JE. It is an attractive candidate for clinical assessment because it is profoundly effective even when given after the inoculation of virus, lacks obvious significant toxic side effects, can be delivered systemically with relatively good CNS penetration, and is reasonably inexpensive.

Acknowledgements

This work is supported by a core Grant from Department of Biotechnology to NBRC. This work was also supported by Grant awarded to AB from the Council of Scientific and Industrial Research (27(0173)/07/EMR-II), Government of India. MKM is a recipient of Senior Research Fellowship from University Grants Commission. We thank Dr Soumya Ghosh, Amit Saxena, and Kanhaiya Lal Kumawat for their help in this study. We thank Professor Vijayalakshmi Ravindranath, Director NBRC for her continuous support and encouragement. The information provided in this study is protected by pending Indian patent (Application No: 211/DEL/2007).

References

Arvin K. L., Han B. H., Du Y., Lin S. Z., Paul S. M. and Holtzman D. M. (2002) Minocycline markedly protects the neonatal brain against hypoxic-ischemic injury. *Ann. Neurol.* **52**, 54–61.

Basu A., Krady J. K., O'Malley M., Styren S. D., DeKosky S. T. and Levison S. W. (2002) The type 1 interleukin-1 receptor is essential for the efficient activation of microglia and the induction of multiple proinflammatory mediators in response to brain injury. *J. Neurosci.* **22**, 6071–6082.

Chen M., Ona V. O., Li M. *et al.* (2000) Minocycline inhibits caspase-1 and caspase-3 expression and delays mortality in a transgenic mouse model of Huntington disease. *Nat. Med.* **6**, 797–801.

Chen C. J., Raung S. L., Kuo M. D. and Wang Y. M. (2002) Suppression of Japanese encephalitis virus infection by non-steroidal anti-inflammatory drugs. *J. Gen. Virol.* **83**, 1897–1905.

Chopra I. (2001) Glycylcyclines: third-generation tetracycline antibiotics. *Curr. Opin. Pharmacol.* **1**, 464–469.

Cohen P. S., Schmidtmayerova H., Dennis J., Dubrovsky L., Sherry B., Wang H., Bukrinsky M. and Tracey K. J. (1997) The critical role of p38 MAP kinase in T cell HIV-1 replication. *Mol. Med.* **3**, 339–346.

Darcissac E. C., Truong M. J., Dewulf J., Mouton Y., Capron A. and Bahr G. M. (2000) The synthetic immunomodulator murabutide controls human immunodeficiency virus type 1 replication at multiple levels in macrophages and dendritic cells. *J. Virol.* **74**, 7794–7802.

Darman J., Backovic S., Dike S., Maragakis N. J., Krishnan C., Rothstein J. D., Irani D. N. and Kerr D. A. (2004) Viral-induced spinal motor neuron death is non-cell-autonomous and involves glutamate excitotoxicity. *J. Neurosci.* **24**, 7566–7575.

Du Y., Ma Z., Lin S. *et al.* (2001) Minocycline prevents nigrostriatal dopaminergic neurodegeneration in the MPTP model of Parkinson's disease. *Proc. Natl Acad. Sci. USA* **98**, 14669–14674.

Fan R., Xu F., Previti M. L., Davis J., Grande A. M., Robinson J. K. and Van Nostrand W. E. (2007) Minocycline reduces microglial activation and improves behavioral deficits in a transgenic model of cerebral microvascular amyloid. *J. Neurosci.* **27**, 3057–3063.

van Genderen H., Kenis H., Lux P., Ungeth L., Maassen C., Deckers N., Narula J., Hofstra L. and Reutelingsperger C. (2006) *In vitro* measurement of cell death with the annexin A5 affinity assay. *Nat. Protoc.* **1**, 363–367.

Ghoshal A., Das S., Ghosh S., Mishra M. K., Sharma V., Koli P., Sen E. and Basu A. (2007) Proinflammatory mediators released by activated microglia induces neuronal death in Japanese encephalitis. *Glia* **55**, 483–496.

Gordon P. H., Moore D. H., Gelinas D. F., Qualls C., Meister M. E., Werner J., Mendoza M., Mass J., Kushner G. and Miller R. G.

(2004) Placebo-controlled phase I/II studies of minocycline in amyotrophic lateral sclerosis. *Neurology* **62**, 1845–1847.

Goswami R., Dawson S. A. and Dawson G. (1998) Cyclic AMP protects against staurosporine and wortmannin-induced apoptosis and opioid-enhanced apoptosis in both embryonic and immortalized (F-11kappa7) neurons. *J. Neurochem.* **70**, 1376–1382.

Hald A. and Lotharius J. (2005) Oxidative stress and inflammation in Parkinson's disease: is there a causal link? *Exp. Neurol.* **193**, 279–290.

Hirsch E. C., Breidert T., Rousselet E., Hunot S., Hartmann A. and Michel P. P. (2003) The role of glial reaction and inflammation in Parkinson's disease. *Ann. NY Acad. Sci.* **991**, 214–228.

Irani D. N. and Prow N. A. (2007) Neuroprotective interventions targeting detrimental host immune responses protect mice from fatal alphavirus encephalitis. *J. Neuropathol. Exp. Neurol.* **66**, 533–544.

Ito T., Deng X., Carr B. and May W. S. (1997) Bcl-2 phosphorylation required for anti-apoptosis function. *J. Biol. Chem.* **272**, 11671–11673.

Jackson A. C., Scott C. A., Owen J., Weli S. C. and Rossiter J. P. (2007) Therapy with minocycline aggravates experimental rabies in mice. *J. Virol.* **81**, 6248–6253.

Kaur R. and Vrati S. (2003) Development of a recombinant vaccine against Japanese encephalitis. *J. Neurovirol.* **9**, 421–431.

Krady J. K., Basu A., Allen C. M., Xu Y., LaNoue K. F., Gardner T. W. and Levison S. W. (2005) Minocycline reduces proinflammatory cytokine expression, microglial activation, and caspase-3 activation in a rodent model of diabetic retinopathy. *Diabetes* **54**, 1559–1565.

Kriz J., Nguyen M. D. and Julien J. P. (2002) Minocycline slows disease progression in a mouse model of amyotrophic lateral sclerosis. *Neurobiol. Dis.* **10**, 268–278.

Krutzik P. O. and Nolan G. P. (2003) Intracellular phospho-protein staining techniques for flow cytometry: monitoring single cell signaling events. *Cytometry A* **55**, 61–70.

Michaelis M., Kleinschmidt M. C., Doerr H. W. and Cinatl J. Jr (2007) Minocycline inhibits West Nile virus replication and apoptosis in human neuronal cells. *J. Antimicrob. Chemother.* **40**, 981–986.

Mishra M. K., Koli P., Bhowmick S. and Basu A. (2007a) Neuroprotection conferred by astrocytes is insufficient to protect animals from succumbing to Japanese encephalitis. *Neurochem. Int.* **50**, 764–773.

Mishra M. K., Koli P., Bhowmick S. and Basu A. (2007b) Neuroprotection conferred by astrocytes is insufficient to protect animals from succumbing to Japanese encephalitis. *Neurochem. Int.* **50**, 764–773.

Nikodemova M., Duncan I. D. and Watters J. J. (2006) Minocycline exerts inhibitory effects on multiple mitogen-activated protein kinases and IkappaBalpha degradation in a stimulus-specific manner in microglia. *J. Neurochem.* **96**, 314–323.

Popovic N., Schubart A., Goetz B. D., Zhang S. C., Linington C. and Duncan I. D. (2002) Inhibition of autoimmune encephalomyelitis by a tetracycline. *Ann. Neurol.* **51**, 215–223.

Richardson-Burns S. M. and Tyler K. L. (2005) Minocycline delays disease onset and mortality in reovirus encephalitis. *Exp. Neurol.* **192**, 331–339.

Sanchez Mejia R. O., Ona V. O., Li M. and Friedlander R. M. (2001) Minocycline reduces traumatic brain injury-mediated caspase-1 activation, tissue damage, and neurological dysfunction. *Neurosurgery* **48**, 1393–1399.

Shapiro L. E., Knowles S. R. and Shear N. H. (1997) Comparative safety of tetracycline, minocycline, and doxycycline. *Arch. Dermatol.* **133**, 1224–1230.

Swarup V., Ghosh J., Ghosh S., Saxena A. and Basu A. (2007a) Antiviral and anti-inflammatory effects of rosmarinic acid in an experimental murine model of Japanese encephalitis. *Antimicrob. Agents Chemother.* **51**, 3367–3370.

Swarup V., Das S., Ghosh S. and Basu A. (2007b) Tumor necrosis factor receptor-1-induced neuronal death by TRADD contributes to the pathogenesis of Japanese encephalitis. *J. Neurochem.* **103**, 771–783.

Thomas M., Le W. D. and Jankovic J. (2003) Minocycline and other tetracycline derivatives: a neuroprotective strategy in Parkinson's disease and Huntington's disease. *Clin. Neuropharmacol.* **26**, 18–23.

Tikka T., Fiebich B. L., Goldsteins G., Keinanen R. and Koistinaho J. (2001) Minocycline, a tetracycline derivative, is neuroprotective against excitotoxicity by inhibiting activation and proliferation of microglia. *J. Neurosci.* **21**, 2580–2588.

Van Den Bosch L., Tilkin P., Lemmens G. and Robberecht W. (2002) Minocycline delays disease onset and mortality in a transgenic model of ALS. *Neuroreport* **13**, 1067–1070.

Vrati S., Giri R. K., Razdan A. and Malik P. (1999a) Complete nucleotide sequence of an Indian strain of Japanese encephalitis virus: sequence comparison with other strains and phylogenetic analysis. *Am. J. Trop. Med. Hyg.* **61**, 677–680.

Vrati S., Agarwal V., Malik P., Wani S. A. and Saini M. (1999b) Molecular characterization of an Indian isolate of Japanese encephalitis virus that shows an extended lag phase during growth. *J. Gen. Virol.* **80**(Pt. 7), 1665–1671.

Wang X., Zhu S., Drozda M., Zhang W., Stavrovskaya I. G., Cattaneo E., Ferrante R. J., Kristal B. S. and Friedlander R. M. (2003) Minocycline inhibits caspase-independent and -dependent mitochondrial cell death pathways in models of Huntington's disease. *Proc. Natl Acad. Sci. USA* **100**, 10483–10487.

Wiesner D. A. and Dawson G. (1996a) Staurosporine induces programmed cell death in embryonic neurons and activation of the ceramide pathway. *J. Neurochem.* **66**, 1418–1425.

Wiesner D. A. and Dawson G. (1996b) Programmed cell death in neurotumour cells involves the generation of ceramide. *Glycoconj. J.* **13**, 327–333.

Wu D. C., Jackson-Lewis V., Vila M., Tieu K., Teismann P., Vadseth C., Choi D. K., Ischiropoulos H. and Przedborski S. (2002) Blockade of microglial activation is neuroprotective in the 1-methyl-4-phenyl-1,2,3,6-tetrahydropyridine mouse model of Parkinson disease. *J. Neurosci.* **22**, 1763–1771.

Yrjanheikki J., Keinanen R., Pellikka M., Hokfelt T. and Koistinaho J. (1998) Tetracyclines inhibit microglial activation and are neuroprotective in global brain ischemia. *Proc. Natl Acad. Sci. USA* **95**, 15769–15774.

Yrjanheikki J., Tikka T., Keinanen R., Goldsteins G., Chan P. H. and Koistinaho J. (1999) A tetracycline derivative, minocycline, reduces inflammation and protects against focal cerebral ischemia with a wide therapeutic window. *Proc. Natl Acad. Sci. USA* **96**, 13496–13500.

Zhu S., Stavrovskaya I. G., Drozda M. *et al.* (2002) Minocycline inhibits cytochrome c release and delays progression of amyotrophic lateral sclerosis in mice. *Nature* **417**, 74–78.

Zink M. C., Uhrlaub J., DeWitt J., Voelker T., Bullock B., Mankowski J., Tarwater P., Clements J. and Barber S. (2005) Neuroprotective and anti-human immunodeficiency virus activity of minocycline. *JAMA* **293**, 2003–2011.

